



University of
Massachusetts
Amherst

Pre-heating By Pre-virialization And Its Impact On Galaxy Formation

Item Type	Article
Authors	Mo, HJ;Yang, XH;van den Bosch, FC;Katz, N;Zehavi, I;Tripp, T;Bowen, DV;Sembach, KR;Jenkins, EB;Savage, BD;Richter, P
DOI	10.1111/j.1365-2966.2005.09512.x
Download date	2026-04-12 00:11:02
Link to Item	https://hdl.handle.net/20.500.14394/2996

Preheating by Previrialization and its Impact on Galaxy Formation

H.J. Mo¹, Xiaohu Yang¹, Frank C. van den Bosch², Neal Katz¹ ^{*}

¹ *Department of Astronomy, University of Massachusetts, Amherst MA 01003-9305, USA*

² *Department of Physics, Swiss Federal Institute of Technology, ETH Hönggerberg, CH-8093, Zurich, Switzerland*

ABSTRACT

We use recent observations of the HI-mass function to constrain galaxy formation. The data conflicts with the standard model where most of the gas in a low-mass dark matter halo is assumed to settle into a disk of cold gas that is depleted by star formation and supernova-driven outflows until the disk becomes gravitationally stable. Assuming a star formation threshold density supported by both theory and observations this model predicts HI masses that are much too large. The reason is simple: supernova feedback requires star formation, which in turn requires a high surface density for the gas. Heating by the UV background can reduce the amount of cold gas in haloes with masses $< 10^{9.5} h^{-1} M_{\odot}$, but is insufficient to explain the observed HI mass function. A consistent model can be found if low-mass haloes are embedded in a preheated medium, with a specific gas entropy ~ 10 keV cm². In addition, such a model simultaneously matches the faint-end slope of the galaxy luminosity function without the need for any supernova driven outflows. We propose a preheating model where the medium around low-mass haloes is preheated by gravitational pancaking. Since gravitational tidal fields suppress the formation of low-mass haloes while promoting that of pancakes, the formation of massive pancakes precedes that of the low-mass haloes within them. We demonstrate that the progenitors of present-day dark matter haloes with $M \lesssim 10^{12} h^{-1} M_{\odot}$ were embedded in pancakes of masses $\sim 5 \times 10^{12} h^{-1} M_{\odot}$ at $z \sim 2$. The formation of such pancakes heats the gas to a temperature of 5×10^5 K and compresses it to an overdensity of ~ 10 . Such gas has a cooling time that exceeds the age of the Universe at $z \lesssim 2$, and has a specific entropy of ~ 15 keV cm², almost exactly the amount required to explain the stellar and HI mass functions.

Key words: dark matter - large-scale structure of the universe - galaxies: haloes - methods: statistical

1 INTRODUCTION

The cold dark matter (CDM) model of structure formation has proven a very successful paradigm for understanding the large-scale structure of the Universe. However, as far as galaxy formation is concerned, a number of important issues still remain. A long-standing problem is that CDM models in general predict too many low-mass dark matter haloes. The mass function of dark matter haloes, $n(M)$, scales with halo mass roughly as $n(M) \propto M^{-2}$ at the low-mass end. This is in strong contrast with the observed luminosity function of galaxies, $\Phi(L)$, which has a rather shallow shape at the faint end, with $\Phi(L) \propto L^{-1}$. To reconcile these observations with the CDM paradigm, the efficiency of star formation must be a strongly nonlinear function of halo mass (e.g.

Kauffmann, White & Guiderdoni 1993; Benson et al. 2003; Yang et al. 2003; van den Bosch et al. 2003b). One of the biggest challenges in galaxy formation is to understand the physical origin of this strongly nonlinear relationship.

Another important but related challenge is to understand the baryonic mass fraction as a function of halo mass. The baryonic mass in dark matter haloes maybe roughly divided into three components: stars, cold gas, and hot gas. In the most naive picture one would expect that each halo has a baryonic mass fraction that is close to the universal value of ~ 17 percent¹. In this naive picture one can achieve a low ratio of stellar mass to halo mass by keeping a relatively large fraction of the baryonic mass hot, either by preventing the gas from cooling or by providing a heat-

^{*} E-mail: hjmo@nova.astro.umass.edu

¹ Corresponding to a Λ CDM concordance cosmology with $\Omega_B h^2 = 0.024$ and $\Omega_m h^2 = 0.14$ (Spergel et al. 2003)

ing source that turns cold gas into hot gas. Alternatively, one may achieve a low star formation efficiency in low-mass haloes by making the total baryonic mass fraction lower in lower mass haloes, which can be achieved either by blowing baryons out haloes or by preventing baryons from ever becoming bound to haloes in the first place.

At the present it is unclear which of these scenarios dominates. To a large extent this ignorance owes to the poor observational constraints on the baryonic inventory as function of halo mass. Historically, most observational studies of galaxies have focussed on the stellar light. Although this has given us a fairly detailed consensus of the relation between stellar mass (or light) and halo mass (e.g., Yang et al. 2003, 2005; van den Bosch et al. 2003b; Tinker et al. 2004), less information is available regarding the hot and cold gas components. Hot, tenuous gas in low mass haloes is notoriously difficult to detect, making our knowledge of the relation between halo mass and hot gas mass quite limited. Based on X-ray observations of a few relatively massive spiral galaxies, the gas mass in a hot halo component appears to be small (e.g. Benson et al. 2000). For cold gas the situation has improved substantially in recent years, owing to the completion of relatively large, blind 21-cm surveys (e.g. Schneider, Spitzak & Rosenberg 1998; Kraan-Korteweg et al. 1999; Rosenberg & Schneider 2002; Zwaan et al. 2003, 2005). Using these surveys, it is now possible to obtain important constraints on galaxy formation (see Section 2).

When modelling galaxy formation, the process most often considered to suppress star formation in low mass haloes is feedback from supernova explosions. As shown by Dekel & Silk (1986) and White & Frenk (1992), the total amount of energy released by supernovae can be significantly larger than the binding energy of the gas in low mass haloes. Therefore, as long as a sufficiently large fraction of this energy can be converted into kinetic energy (often termed the ‘feedback efficiency’), one can in principle expel large amounts of baryonic material from low mass haloes, thus reducing the efficiency of star formation. Indeed, semi-analytical models for galaxy formation that include a simple model for this feedback process are able to reproduce the observed slope of the faint-end luminosity function in the standard Λ CDM model, if the feedback efficiency is taken to be sufficiently high (e.g., Benson et al. 2003; Kang et al. 2005).

An important question, however, is whether such high efficiencies are realistic. For example, detailed hydrodynamical simulations by Mac-Low & Ferrara (1999) and Strickland & Stevens (2000) show that supernova feedback is far less efficient in expelling mass than commonly assumed because the onset of Rayleigh-Taylor instabilities severely limits the mass loading efficiency of galactic winds.

This prompted investigations into alternative mechanisms to lower the star formation efficiency in low mass haloes. Another possibility is that photoionization heating by the UV background may prevent gas from cooling into low-mass haloes (e.g., Efstathiou 1992; Thoul & Weinberg 1996) by increasing its temperature. Numerical simulations have shown that this effect is only efficient in dark matter haloes with $M \lesssim 10^{10} h^{-1} M_{\odot}$ (e.g. Quinn et al. 1996, Gnedin 2000; Hoeft et al. 2005), since the gas is only heated to $\sim 10^4$ to 10^5 K. Although this might be sufficient to explain the relatively low abundance of satellite galaxies in Milky Way sized haloes (Bullock, Kravtsov & Weinberg 2000; Tully et

al. 2002), it is insufficient to explain the faint-end slope of the galaxy luminosity function. However, if a different mechanism were to heat the intergalactic medium (hereafter IGM) to even higher temperatures (and thus higher entropies), the same mechanism could affect more massive haloes as well. Such a process is often referred to as ‘preheating’. Along these lines, Mo & Mao (2002) considered galaxy formation in an IGM that was preheated to high entropy by vigorous energy feedback associated with the formation of stars in old ellipticals and bulges and with active galactic nuclei (AGN) activity at redshifts of 2 to 3. They showed that such a mechanism can produce the entropy excess observed today in low-mass clusters of galaxies without destroying the bulk of the Ly- α forest. In addition, it would affect the formation of galaxies in low mass haloes whose virial temperature is lower than that of the preheated IGM. Numerical simulations show that such preheating may indeed significantly lower the gas mass fraction in low mass haloes (e.g., van den Bosch, Abel & Hernquist 2003a; Lu et al. in preparation).

In this paper we investigate an alternative mechanism for creating a preheated IGM. Rather than relying on star formation or AGN, we consider the possibility that the collapse of pancakes (also called sheets) and filaments heats the gas in these structures and that the low mass haloes within them form in a preheated medium. Although the standard picture of hierarchical formation is one in which more massive structures form later, gravitational tidal fields suppress the formation of low-mass haloes, while promoting the formation of pancakes. Consequently, the formation of massive pancakes will precede that of low-mass dark matter haloes, which form within them. In this paper we show that the shock heating associated with pancake collapse at $z \lesssim 2$ can heat the associated gas to sufficiently high entropy that the subsequent gas accretion into the low mass haloes that form within these pancakes is strongly affected. We demonstrate that the impact of this previrialization is strong enough to explain both the faint-end of the galaxy luminosity function and the low mass end of the galaxy HI mass function, without having to rely on unrealistically high efficiencies for supernova feedback.

The outline of the paper is as follows. In § 2, we use current observational results of the HI gas mass function to constrain star formation and feedback in low-mass haloes. We show that these observations are difficult to reconcile with the conventional feedback model, but that a consistent model can easily be found if low-mass haloes are embedded in a preheated medium. In § 3 we describe how shocks associated with the formation of pancakes can preheat the gas around low-mass haloes. In § 4 we discuss our results in light of existing numerical simulations and discuss the impact of our results on the properties of galaxies and the intergalactic medium. We summarize our results in § 5.

2 THE FORMATION OF DISK GALAXIES

2.1 Observational Constraints

The models discussed below focus on galaxies that form at the centers of relatively low mass haloes with $M \lesssim 10^{12} h^{-1} M_{\odot}$. To constrain these models, we first derive the stellar mass function of central galaxies using the conditional luminosity function (CLF), which expresses how many

galaxies of luminosity L reside, on average, in a halo of mass M . Using both the galaxy luminosity function and the luminosity dependence of the correlation length of the galaxy-galaxy correlation function obtained from the 2-degree Field Galaxy Redshift Survey (2dFGRS, Colless et al. 2001), Yang et al. (2003) and van den Bosch et al. (2003b) were able to put tight constraints on the CLF (see also Yang et al. 2005 and van den Bosch et al. 2005). As shown in Yang et al. (2003), the CLF also allows one to compute the average relation between halo mass and the luminosity of the central galaxy (assumed to be the brightest galaxy in the halo). We have determined this relation using the fiducial CLF model considered in van den Bosch et al. (2005; Model 6 listed in their Table 1). To obtain a stellar mass function for the central galaxies, we convert the 2dFGRS b_J -band luminosity into a stellar mass using a stellar mass-to-light ratio $M_{\text{star}}/L = 4.0 (L/L^*)^{0.3} (M/L)_{\odot}$ for $L \leq L^*$ and $M_{\text{star}}/L = 4.0(M/L)_{\odot}$ for $L > L^*$, which matches the mean relation between stellar mass and blue-band luminosity obtained by Kauffmann et al. (2003). The resulting stellar mass function of central galaxies is shown in Fig. 1(a) as the short-dashed curve. For comparison, we also plot the stellar mass functions of *all* galaxies obtained by Bell et al. (2003) (dotted curve) and Panter, Heavens & Jimenez (2004) (long-dashed curve). Given the large uncertainties involved (see Bell et al. 2003 for a detailed discussion), these stellar mass functions are in remarkably good agreement with each other, particularly for the low mass galaxies that are the focus of this study. The good agreement suggests that most low mass galaxies are indeed central galaxies in small haloes, i.e. satellite galaxies do not dominate the stellar mass function (see also Cooray & Milosavljević 2005).

In addition to the stellar mass function, we also constrain our models using the HI mass function of galaxies. With large, blind 21-cm surveys that have recently been completed, this HI-mass function has now been estimated quite accurately over a relatively large range of masses (see Zwaan et al. 2005 and references therein). In Fig. 1(b), we show the recent results obtained by Zwaan et al. (2005) and Rosenberg & Schneider (2002). Both HI-mass functions are well fit by a Schechter (1976) function with a power-law slope at the low mass end of about -1.3 ± 0.1 . Note that this is slightly steeper than the power-law slope at the low mass end of the stellar mass function, which is about -1.16 (Panter et al. 2004). Since galaxy formation is a process that involves both stars and cold gas, a combination of observational constraints on the luminosity function and the HI-mass function provides important constraints on star formation and feedback. In fact, as we show below, the HI-mass function constraints are more generic, and it is only by including them we are able to argue against the standard supernova feedback model.

2.2 The standard model

In the standard picture of galaxy formation (White & Rees 1978) it is assumed that gas cooling conserves specific angular momentum. As a result, the baryons cool to form a centrifugally supported disk galaxy (Fall & Efstathiou 1980). In what follows we investigate the mass functions of the cold gas and stars of disk galaxies that form within this picture. We make the simplifying assumption that each dark mat-

ter halo forms a single disk galaxy. Clearly this is a severe oversimplification since it is known that haloes, especially more massive ones, can contain more than one galaxy and not every galaxy is a disk galaxy. However, we are only interested in the properties of low mass haloes, which to good approximation contain a single, dominant disk galaxy. In particular, the studies of van den Bosch et al. (2003b), Yang et al. (2005), and Weinmann et al. (2005) show that in haloes with $M < 10^{12} h^{-1} M_{\odot}$, the mass range considered here, the fraction of late-type galaxies is larger than 60 percent (see also Berlind et al. 2003). Thus, our simplified model will overpredict the number density of disk galaxies in low mass haloes, but not by more than a factor of two. Furthermore, we will conclude below that the main problem with the standard model is one of gas cooling, a problem that will exist independent of galaxy type.

To model the detailed structure of individual disk galaxies we use the model of Mo, Mao & White (1998, hereafter MMW), which matches a wide variety of properties of disk galaxies. Specifically, this model assumes that (i) the baryons have the same specific angular momentum as the dark matter, (ii) they conserve their specific angular momentum when they cool, (iii) they form an exponential disk, and (iv) the halo responds to the gas cooling by adiabatically contracting. Assumptions (i) and (iv) are supported by numerical simulations (van den Bosch et al. 2002; Jesseit, Naab & Burkert 2002), while assumption (ii) is required to obtain disks of the right size. Finally, assumption (iii) is equivalent to assuming a particular distribution of specific angular momentum in the proto-galaxy. Haloes are modelled as NFW spheres (Navarro, Frenk & White 1997) with a concentration that depends on halo mass following Bullock et al. (2001a), and a halo spin parameter, λ , that is drawn from a lognormal distribution with a median of ~ 0.04 and a dispersion of ~ 0.5 (e.g., Warren et al. 1992; Cole & Lacey 1996; Bullock et al. 2001b). The one free parameter in this model is the disk mass fraction m_d , defined as the disk mass divided by the total virial mass. Since radiative cooling is very efficient in low mass haloes with $M < 10^{12} h^{-1} M_{\odot}$, we start our investigation by naively setting m_d equal to the universal baryon fraction, i.e., $m_d = 0.17$.

In a seminal paper, Kennicutt (1989) showed that star formation is abruptly suppressed below a critical surface density. This critical density is close to that given by Toomre's stability criterion

$$\Sigma_{\text{crit}}(R) = \frac{\sigma_{\text{gas}} \kappa(R)}{\pi G Q_{\text{crit}}}, \quad (1)$$

where $\kappa(R)$ is the epicyclic frequency, σ_{gas} is the velocity dispersion of the cold gas and $Q_{\text{crit}} \sim 1$ (Toomre 1964). This critical density determines the fraction of the gas that can form stars (Quirk 1972). Given the surface density of the disk, Σ_{disk} , obtained using the MMW model described above, the radius R_{SF} where the density of the disk equals Σ_{crit} can be calculated. Following van den Bosch (2000) we assume that the disk mass inside this radius with surface density $\Sigma_{\text{disk}} > \Sigma_{\text{crit}}$ turns into stars, i.e.

$$M_{\text{star}} = 2\pi \int_0^{R_{\text{SF}}} [\Sigma_{\text{disk}}(R) - \Sigma_{\text{crit}}(R)] R dR \quad (2)$$

Kennicutt (1989) shows that $\sigma_{\text{gas}} = 6 \text{ km s}^{-1}$ and $Q_{\text{crit}} \sim 1.5$ yields values of R_{SF} that correspond roughly to the radii

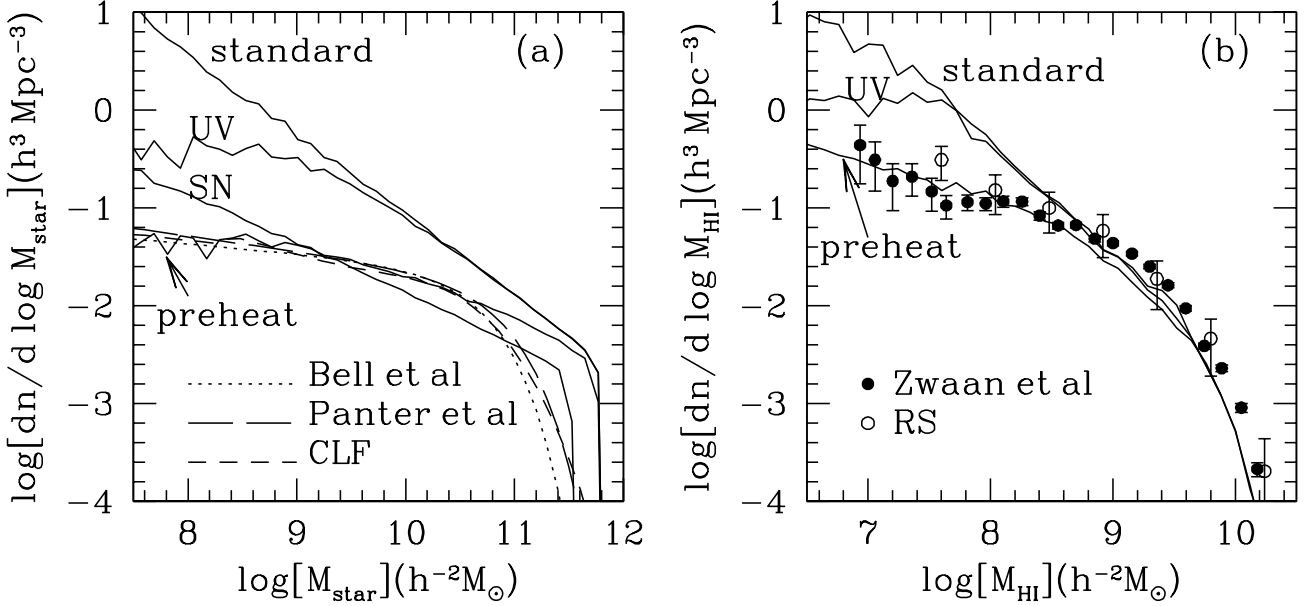


Figure 1. (a) The stellar mass functions predicted by the standard model, the model with heating by the UV background, and the preheating model, as labelled. The curve labelled ‘SN’ is the prediction of a model in which cold gas is heated by supernova explosions (see text for details). In addition, we show the observational results of Bell et al. (2003; dotted curve) and Panter et al. (2004; long-dashed curve), as well as the stellar mass function of *central* galaxies in dark matter haloes derived from the CLF as described in the text (short-dashed curve). (b) The HI-mass functions predicted by the same three models compared to the observed HI mass functions of Rosenberg & Schneider (2002; RS, open circles) and Zwaan et al. (2005; solid dots).

where star formation is truncated. However, Hunter et al (1998) show that in low surface brightness galaxies $Q_{\text{crit}} \sim 0.75$. Therefore, to be conservative, we adopt $\sigma_{\text{gas}} = 6 \text{ km s}^{-1}$ and $Q_{\text{crit}} \sim 0.75$. The assumption that *all* the gas with $\Sigma_{\text{disk}} > \Sigma_{\text{crit}}$ has formed stars is consistent with both observations (Kennicutt 1989; Martin & Kennicutt 2001; Wong & Blitz 2002; Zasov & Smirnova 2005) and with predictions based on the typical star formation rate in disk galaxies (Kennicutt 1998) and their formation times (see van den Bosch 2001). We compute the gas mass of each model galaxy using $M_{\text{gas}} = (M_{\text{disk}} - M_{\text{star}})$ where $M_{\text{disk}} = m_d M$. In other words, we assume that the gas surface density $\Sigma_{\text{gas}} = \Sigma_{\text{crit}}$ inside R_{SF} and $\Sigma_{\text{gas}} = \Sigma_{\text{disk}}$ outside R_{SF} . Finally, again to be conservative, we assume that the molecular hydrogen fraction is 1/2 (e.g. Keres et al 2003; Boselli et al. 2002) so that the final HI mass of each galaxy, $M_{\text{HI}} = 0.71 M_{\text{gas}}/2$ where the factor of 0.71 takes into account the contribution of helium and other heavier elements.

Using the halo mass function given by the Λ CDM concordance cosmology, and assuming that each halo hosts a single disk galaxy whose properties follow from M , m_d , and λ as described above, we obtain the HI and stellar mass functions shown as the solid curves labeled ‘standard’ in Figure 1. Since we are only interested in low-mass haloes, and since our model does not include any processes that may affect gas assembly in massive haloes, we artificially truncate the halo mass function at $M = 5 \times 10^{12} h^{-1} M_{\odot}$, which explains the abrupt turnover of the model’s stellar mass function at high masses. Not surprisingly, our naive model severely overpredicts the stellar mass function, yielding an abundance of systems with $M_{\text{star}} \simeq 10^8 h^{-2} M_{\odot}$ that is two orders of magnitude too large. In addition, the model

predicts an HI mass function at $M_{\text{HI}} \lesssim 10^8 h^{-2} M_{\odot}$ that is more than 10 times higher than the data. Even if we reduce the number density of dark matter haloes by a factor of 2, to account for the possibility that some isolated haloes may not host disk galaxies, the discrepancy remains a factor of five. Note that one might try to lower the stellar masses in our model by increasing Σ_{crit} , but this leads to an increase of the HI masses, which are already too large. Similarly, a decrease of Σ_{crit} may improve the fit of the HI mass function, but at the expense of worsening the fit to the stellar mass function. The failure of the standard model to simultaneously fit the HI mass function and the stellar mass function is robust to the details of star formation. Fitting both mass functions simultaneously requires either a modification of the cosmological parameters or additional physics to lower m_d . In what follows, we consider both these possibilities separately.

2.3 Cosmological Parameters

One of the main reasons that the predicted HI mass function is very steep at the low-mass end is that the halo mass function predicted by the standard Λ CDM model is also very steep at the low-mass end. Hence, one way to alleviate the discrepancy between the model and observations is to change the cosmological parameters such that the low-mass slope of the halo mass function becomes shallower. Unfortunately, the steep halo mass function is a very generic property of all CDM models. In particular, the slope at the low-mass end is almost independent of cosmological parameters, including the cosmic density parameter and the amplitude of the primordial perturbations. The only way to change the slope of the mass function at the low-mass end is to as-

sume that the effective power index of the primordial density perturbation spectrum is significantly lower than the scale invariant value. However, such models are not favored by the power spectrum derived directly from the temperature fluctuations of the cosmic microwave background and the Lyman- α forest (e.g., Croft et al. 1999; Seljak et al. 2003), and are difficult, if not impossible, to reconcile with inflation. Another possibility is that the universe is dominated by warm dark matter (WDM) instead of CDM, so that the power spectrum on small scales is suppressed by free stream damping of the WDM particles. Here again observations of the Lyman- α forest provide a stringent constraint on the particle mass (Narayanan et al. 2000). With particle masses in the allowed range, the WDM model yields a halo mass function that is virtually indistinguishable from that of the CDM models in the halo mass range considered here. In other words, within the parameter space allowed by the data, modifications of the cosmological parameters do not have any significant impact on the results of the standard model presented above.

2.4 Supernova Feedback

Thus far we have only considered models in which the disk mass fraction is equal to the universal baryon fraction, i.e. where $m_d = 0.17$. We now consider physical mechanisms that can lower m_d , and investigate whether this allows a simultaneous match of the HI and stellar mass functions. We first consider what has become the standard mechanism, namely feedback by supernovae. In this model each halo acquires a baryonic mass fraction that is equal to the universal value (0.17) but m_d is reduced since supernovae inject large amounts of energy into the cold gas, causing it to be ejected from the galaxy.

In semi-analytical models of galaxy formation, two schemes have been proposed to model this supernova feedback. In the ‘retention’ model considered by Kauffmann et al. (1999), Cole et al. (2000), Springel et al. (2001) and Kang et al. (2005), among others, part of the cold gas in a galaxy disk is assumed to be heated by supernovae to the halo virial temperature and is added to the hot halo gas for cooling in the future. Since radiative cooling is effective in galaxy haloes, the feedback efficiency must be high enough to keep a large amount of the gas in the hot phase (Benson et al. 2003). However, if there is a critical surface density below which star formation ceases, no galaxy disk is expected to have a surface density below this critical density, because otherwise the feedback from star formation would be insufficient to keep most of the gas hot. We plot an example of such a model in Figure 1. In this model we make the standard assumption that the rate at which cold gas is heated by supernova explosions is proportional to the star formation rate, $\dot{M}_{\text{reheat}} = \beta \dot{M}_*$, where $\beta = (V_{\text{hot}}/V_c)^2$, with V_c the circular velocity of the host halo, and V_{hot} an adjustable parameter (e.g. Benson et al. 2003). If the heated gas is not able to cool, the mass of the gas that can form stars will be $1/(1 + \beta)$ times $m_d M - M_{\text{gas}}$, where M_{gas} is the mass of the gas that remains in the disk. The curve labelled ‘SN’ in Figure 1 is the result corresponding to $V_{\text{hot}} = 280 \text{ km s}^{-1}$. Although the stellar mass function is reduced significantly in this model, the predicted slope at the low-mass end is much too steep. Furthermore, the HI-mass function is un-

changed from the standard no-feedback model and so it is still unable to match the observed HI-mass function. In addition, this model predicts fairly extensive haloes of hot, X-ray emitting gas, which is inconsistent with observations (Benson et al. 2000).

An alternative feedback model, considered by Kauffmann et al. (1999) and Somerville & Primack (1999), is the ‘ejection’ model in which the reheated gas is assumed to be ejected from the current host halo. If the initial velocity of the ejected gas is not much larger than the escape velocity of the host halo, the gas will be recaptured at a later epoch as the halo grows more massive by accreting new material from its surroundings. Then, as in the retention model, the baryon fraction in the more massive halo will be similar to the universal value, except that a (typically small) delay time is added. Consequently, this model also cannot produce disks with gas surface densities below the critical density, which again results in a severe overproduction of low HI mass systems. Only if the supernova explosion energy heats the cold gas to an energy much greater than the binding energy of the halo can the wind escape the halo forever and potentially reduce the number of low HI mass systems. However, there are several problems with this scenario. First, as shown by Martin (1999) and Heckman et al. (2000), the observed mass outflow rate in starburst galaxies, which are extreme systems, is about twice the star formation rate. This implies that one can never achieve a disk mass fraction that is lower than about 1/3 the universal baryon fraction, which is not nearly enough to match the HI observations. Second, the numerical simulations of Mac-Low & Ferrara (1999) and Strickland & Stevens (2000) have shown that the mass loss rates in quiescent disk galaxies are much lower than those observed in starburst galaxies. Third, as shown in Benson et al. (2003), the feedback efficiencies that are required to permanently eject the gas are completely unphysical. Finally, as shown in van den Bosch (2002), even if one ignores all these problems and simply ejects the gas forever, the presence of a star formation threshold density still assures that the final surface density of the gas is similar to the critical surface density. As is evident from Figure 5 in that paper, supernova feedback that is modelled with permanent ejection has a drastic impact on the stellar masses but leaves the gas mass basically unchanged. Again, this owes to the fact that gas ejection requires supernovae, which in turn requires star formation, which requires a gas surface density that exceeds the critical density. Note that although supernova feedback may temporarily deplete the gas surface density below the critical value, the ongoing cooling of new and previously expelled material will continue to increase the cold gas surface density until it exceeds Σ_{crit} , initiating a new episode of star formation and its associated feedback. As shown in van den Bosch (2002), this results in a population of disk galaxies whose cold gas surface densities are, in a statistical sense, similar to Σ_{crit} .

In summary, although supernova feedback may be tuned to yield a good match to the low-mass end of the stellar mass function, it has three fundamental problems: (i) the efficiency needed seems unphysically high compared to what it achieved in detailed numerical simulations, (ii) unless the hot gas is expelled from the halo indefinitely it predicts haloes of hot, X-ray emitting gas which are inconsistent with observations, and (iii) as demonstrated here,

if one takes account of a star formation threshold density, which is strongly supported by both theory and observations, it overpredicts the abundance of systems with low HI masses by almost an order of magnitude. In short, the problem of matching the observed HI mass functions is one of preventing gas from entering the galaxy in the first place. Standard feedback schemes fail because even if all the gas is temporarily removed, e.g. by a massive supernova outflow, it will just reaccrete more gas. This is also why our arguments, although framed around disk galaxies, should hold for all galaxies. It is, therefore, important to seek other solutions that are physically more plausible.

2.5 Reionization and Preheating

In the models considered above we assume that the IGM accreted by the dark matter haloes is cold, allowing all of the gas originally associated with the halo to be accreted eventually. However, if the gas in the IGM is preheated to a specific entropy that is comparable to or larger than that generated by the accretion shocks associated with the formation of the haloes, not all of this gas will be accreted into the halo (e.g. Mo & Mao 2002; Oh & Benson 2003; van den Bosch et al. 2003a). In that case, some disks may start with a gas surface density already below the critical density, making their HI gas masses smaller. Note that this circumvents the problem with the supernova feedback scenario that requires star formation and its inherent high gas surface densities.

Let us first consider photoionization heating by the UV background. After reionization, the UV background can heat the IGM to a temperature of roughly 20,000K. As first pointed out by Blumenthal et al. (1984), such heating of the IGM can affect gas accretion into dark matter haloes of low masses (see also Rees 1986; Efsthathiou 1992; Quinn et al. 1996; Thoul & Weinberg 1996). Recent simulations (e.g., Gnedin 2000; Hoesft et al. 2005) follow the detailed evolution of the UV background and show that at the present time the fraction of gas that can be accreted into a dark matter halo of mass M can be written approximately as

$$m_{\text{gas}} = \frac{f_B}{(1 + M_c/M)^\alpha}, \quad (3)$$

where f_B is the universal baryon fraction. Following Hoesft et al. (2005), we consider a model with $M_c = 1.7 \times 10^9 h^{-1} M_\odot$, and $\alpha = 3$. Using the same disk formation model as described in Section 2.2, and assuming that disks with surface densities below Σ_{crit} do not form any stars, we can predict the cold gas and stellar masses. The resulting stellar and HI-mass functions are shown as the solid lines labelled ‘UV’ in Figure 1. Although preheating by the UV background clearly reduces both the stellar and HI-mass functions at the low-mass end, the strength of the effect fails to reconcile the models with the data (see also Benson et al. 2002).

However, since the predicted cold gas mass is significantly reduced in haloes with masses below the characteristic mass scale M_c , this motivated us to consider a model in which the IGM around low-mass haloes is preheated to a temperature that is significantly higher than 20,000K. A higher temperature corresponds to a larger M_c . As shown in Lu & Mo (2005, in preparation), the mass fraction of baryons that are accreted by dark matter haloes

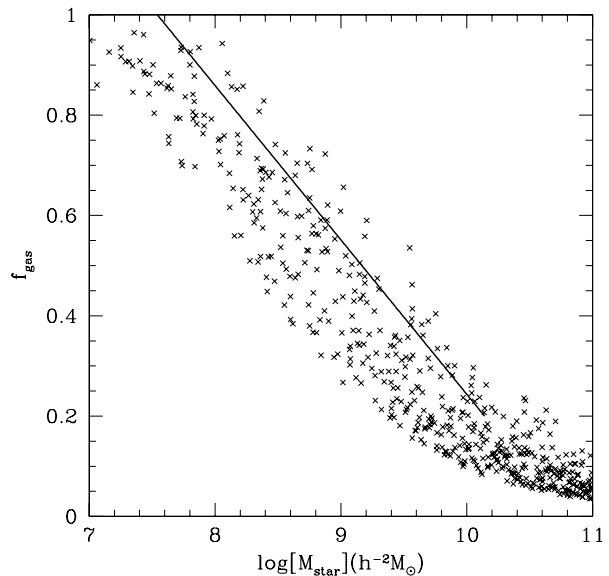


Figure 2. The cold gas mass fraction, defined as the ratio between the mass of cold gas and the total mass of stars and cold gas, as a function of stellar mass predicted by the preheating model (crosses). The thick solid line shows the observed mean relation given by McGaugh & de Blok (1997).

in a strongly preheated medium is well described by equation (3) with $\alpha \sim 1$. Therefore, as a test of this idea we adopt $\alpha = 1$ and choose $M_c = 5 \times 10^{11} h^{-1} M_\odot$, which corresponds to an initial specific entropy for the preheated IGM of $s \equiv T/n_e^{2/3} \sim 10 \text{ keV cm}^2$ (where n_e is the number density of electrons). To determine the relationship between M_c and s we assume that T is the virial temperature of a halo with mass M_c at the present time and that n_e is the mean density of electrons within the halo. In §3, we propose a model that explains how the IGM is preheated to such a level. Here we examine how this preheating affects both the HI-mass function and the stellar mass function

The solid curves labelled ‘preheat’ in Figure 1 show the stellar and HI-mass functions predicted by this model, using the same disk formation model described above. Contrary to the standard model and the reionization model, this preheating model agrees with the data fairly well for the low mass haloes that concern us here. We underpredict the HI mass function at higher masses but remember to be conservative we tried to make the HI mass function as small as possible. For example, we took a small value $Q_{\text{crit}} = 0.75$, which is appropriate for dwarf galaxies. If we took $Q_{\text{crit}} \sim 1.5$, which is appropriate for larger galaxies, it would increase the masses and make them better match the observations.

Unlike the supernova feedback model, preheating can simultaneously match the HI and stellar mass functions. However, this does not guarantee that the model also predicts the correct ratio of cold gas mass to stellar mass in individual galaxies. To test this, we compute for each model galaxy the cold gas mass fraction, $f_{\text{gas}} \equiv M_{\text{gas}}/(M_{\text{gas}} + M_{\text{star}})$. Figure 2 plots f_{gas} as a function of the stellar mass. The scatter in the model predictions results from the scatter in the halo spin parameters, and is comparable to the observed scatter (McGaugh & de Blok 1997). The preheating model predicts that the gas mass fraction decreases with stellar mass, in

qualitative agreement with the observations (McGaugh & de Blok 1997; Garnett 2002). As already demonstrated in van den Bosch (2000), this success is a direct consequence of implementing a critical surface density for star formation. Note that the model predicts gas fractions that are slightly lower than those observed. However, given the uncertainties involved, both in the data and in the model, and given the relatively large amount of scatter, we do not consider this a serious shortcoming.

As a final test of the preheating model we consider gas metallicities. The higher gas mass fractions in smaller haloes implies that the metallicity of the cold gas must be lower in lower mass systems, which is consistent with observations (Garnett 2002). However, observations also show that the *effective* metal yield decreases with galaxy luminosity (Garnett 2002; Tremonti et al. 2004), suggesting that some metals generated by stars must have been ejected from the galaxies and that the ejected fraction is larger for fainter galaxies. This may seem problematic for the preheating model considered here, since we require no outflows to match the HI and the stellar mass functions. However, this does not exclude the possibility that significant amounts of *metals* have been ejected from low-mass galaxies. In fact, as the numerical simulations of Mac-Low & Ferrara (1999) demonstrate, supernova feedback in quiescent disk galaxies is far more efficient at ejecting metals than mass. The reason for this is that the metals are largely produced by the supernovae themselves, so they are part of the hot bubbles of tenuous gas that make up the galactic winds. When these bubbles rupture owing to Raleigh-Taylor instabilities this strongly metal enriched material, which has relatively little mass, is blown away from the disk by its own pressure. Thus, although clearly more work is needed to test this in detail, we believe that the observed effective metal yields are not at odds with the preheating model.

3 PREHEATING BY GRAVITATIONAL PANCAKING

In the previous section we have shown that a preheating model, in which the gas surrounding present-day low mass haloes is preheated to a specific entropy of $s \sim 10 \text{ keV cm}^2$, can simultaneously match the low mass ends of both the HI-mass function and the stellar mass function. Here we propose a physical process that can cause such preheating.

We base our proposed model on the following considerations. In the basic picture of structure formation in CDM cosmologies, as the universe expands, larger and larger objects collapse owing to gravitational instability. The collapse is generically aspherical (Zel'dovich 1970), first forming sheet-like pancakes (first axis collapse), followed by filamentary structures (second axis collapse), and eventually virialized dark matter haloes (third axis collapse). Thus, according to the ellipsoidal collapse model, the formation of a virialized halo requires the collapse of all three axes (e.g. Bond & Myers 1996; Sheth, Mo & White 2001). However, owing to the large scale tidal field, the density threshold for the formation of a low-mass halo, i.e. one with a mass below the characteristic mass, M_* , defined as the mass at which the rms fluctuation is equal to unity, can be much higher than that in the spherical collapse model. This de-

lays the formation of low mass haloes relative to the prediction of the spherical collapse model. Conversely, the tidal field accelerates the collapse of the first (shortest) axis and hence the formation of a pancake can require a density threshold much lower than that for spherical collapse. Consequently, many of today's low mass haloes, i.e. those with $M \ll M_*(z=0) \sim 10^{13} h^{-1} M_\odot$, formed in pancakes of larger mass, which formed before the haloes themselves.

In the process of pancake formation, the gas associated with the pancake is shock heated. If the temperature of the shocked gas is sufficiently high, and if the gas is not able to cool in a Hubble time, the haloes embedded in the pancakes will have to accrete their gas from a preheated medium, which as we showed in the previous section may have important implications for the formation of galaxies within those haloes. To see if this process of ‘‘gravitational pancaking’’ (or previrialization, Peebles 1990) can generate a preheated medium with the required specific entropy, we need to examine the properties of the pancakes within which present-day low mass haloes formed, and to understand how the gas associated with these pancakes was shock heated.

To study the first problem it is important to realize that the bias parameters of haloes with $M \lesssim 0.1 M_*$ have similar values (Mo & White 1996; 2002; Jing 1999; Sheth & Tormen 1999; Sheth, Mo & Tormen 2001; Seljak & Warren 2004; Tinker et al. 2004). This means that all such haloes are, in a statistical sense, embedded within similar large-scale environments. At $z=0$, $M_* \sim 10^{13} h^{-1} M_\odot$, and so all haloes with $M \lesssim 10^{12} h^{-1} M_\odot$ are embedded within similar environments.

According to the ellipsoidal collapse model, the collapse of a region on some mass scale M in the cosmic density field is specified by δ , the average overdensity of the region in consideration, and by e and p , which express the ellipticity and prolateness of the tidal shear field in the neighborhood of that region. According to Sheth et al. (2001), the density threshold for the formation of a virialized halo is given by solving

$$\frac{\delta_{\text{ec}}(e, p)}{\delta_{\text{sc}}} = 1 + \beta \left[5(e^2 \pm p^2) \frac{\delta_{\text{ec}}^2(e, p)}{\delta_{\text{sc}}^2} \right]^\gamma, \quad (4)$$

where $\beta = 0.47$, $\gamma = 0.615$, and δ_{sc} is the critical overdensity for spherical collapse. For a Gaussian density field, the joint distribution of e and p for given a δ is

$$g(e, p|\delta) = \frac{1125}{\sqrt{10\pi}} e (e^2 - p^2) \left(\frac{\delta}{\sigma} \right)^5 e^{-5\delta^2(3e^2+p^2)/2\sigma^2}, \quad (5)$$

where σ is the rms fluctuation of the density field on the mass scale in consideration (Doroshkevich 1970). For all e , this distribution peaks at $p=0$, and the maximum occurs at

$$e_{\text{max}}(p=0|\delta) = \frac{\sigma}{\sqrt{5\delta}}. \quad (6)$$

Thus, the most probable value of e is related to the mass scale through σ . Using this relation, one can obtain a relation between the density threshold for collapse and the halo mass:

$$\delta_{\text{ec}}(M, z) = \delta_{\text{sc}}(z) \left\{ 1 + 0.47 \left[\frac{\sigma^2}{\delta_{\text{sc}}^2(z)} \right]^{0.615} \right\} \quad (7)$$

(Sheth et al. 2001).

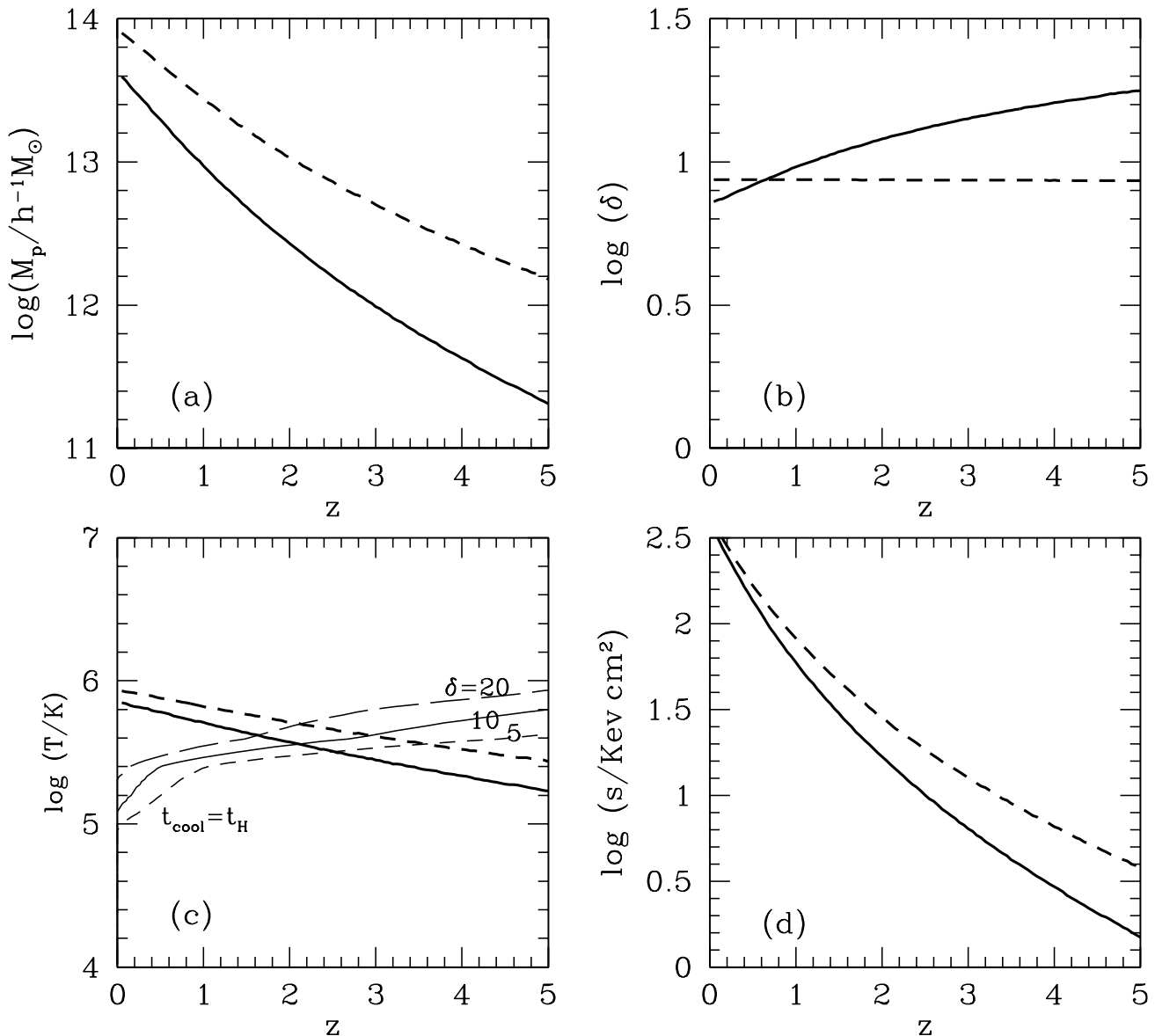


Figure 3. The mass [panel (a)], overdensity [panel (b)], gas temperature [panel (c)], and gas specific entropy [panel (d)] of pancakes around low-mass haloes at the time of first axis collapse. Thick solid curves assume that perturbations around low-mass haloes have e values equal to the most probable values corresponding to the mass scale in consideration, while thick dashed curves show the results in which e is assumed to be a constant, i.e. independent of pancake mass. The thin lines in panel (c) show the loci of $t_{\text{cool}} = t_{\text{H}}$ for the three indicated values of the overdensity.

The ellipsoidal collapse model can also be used to determine the density threshold for the formation of pancakes. Based on similar considerations, one can obtain a corresponding relation between the collapse density threshold and the mass of the pancake:

$$\delta_{\text{ec}}(M, z) = \delta_{\text{sc}}(z) \left\{ 1 - 0.56 \left[\frac{\sigma^2}{\delta_{\text{sc}}^2(z)} \right]^{0.55} \right\} \quad (8)$$

(Shen, Abel, Mo & Sheth, in preparation). As one can see, for low peaks (i.e. $\delta_{\text{sc}}/\sigma \ll 1$), the two thresholds can be very different, while for high peaks they are similar. Thus, the effect of pancaking on subsequent halo formation is more

important for lower peaks, i.e. for lower mass haloes with later formation times.

Given the above properties of the collapse thresholds, we are able to address the following question: for low-mass haloes identified at the present time, what is the nature of the pancakes within which their progenitor haloes were embedded at an earlier time? To quantify the formation of pancakes around a given halo rigorously, one needs to calculate the conditional probability distribution for the overdensity of density perturbations on various scales around the halo and the corresponding tidal shear fields. It is beyond the scope of this paper to present such a detailed analysis here. Instead, we use the cross-correlation between haloes and the

linear density field to determine the average linear overdensity around dark matter haloes on different scales. We then use this overdensity to characterize the mean environment of haloes of a given mass at the present time at earlier times.

According to the halo bias model (Mo & White 1996), the average linear overdensity within a radius r of a halo of mass M can be written as

$$\bar{\delta}_l(r) = b(M)\bar{\xi}_m(r), \quad (9)$$

where $b(M)$ is the bias parameter for haloes of mass M , and the average two-point correlation function of the linear density field

$$\bar{\xi}_m(r) \equiv \frac{3}{r^3} \int_0^r \xi_m(r')r'^2 dr', \quad (10)$$

where $\xi_m(r)$ is the two-point correlation function. The radius r corresponds to a mass scale $M_r = (4\pi r^3/3)\bar{\rho}_0$, where $\bar{\rho}_0$ is the mean density of the universe at $z = 0$. As we mentioned above, the bias parameter for present day haloes with $M \lesssim 10^{12} h^{-1} M_\odot$ is independent of halo mass, with $b \sim 0.65$ (Sheth et al. 2001; Jing 1999; Seljak & Warran 2004; Tinker et al. 2004). We adopt this value to calculate $\bar{\delta}_l$. It is then straightforward to calculate the linear overdensity $\bar{\delta}_l$ as a function of r and the corresponding mass scale M_r . If this overdensity reaches the overdensity threshold for pancake formation at a given redshift, a pancake of mass M_r will form. Since the overdensity threshold depends on the values of p and e , in principle one has to calculate the joint distribution function of e and p for the appropriate mass and overdensity, under the condition that the region contains a halo of mass M at the present time. As an approximation, we assume that both e and p take their most probable values on the mass scale in question, so that $p = 0$ and $e = e_{\max}$. We expect this approximation to be valid for $M_r \gg M$, where the correlation between the properties of the halo and its environment becomes weak (e.g. Bardeen et al. 1986).

For a given $\bar{\delta}_l$, M_r , p and e , we use the ellipsoidal collapse model described in Bond & Myers (1996) to follow the collapse of a uniform ellipsoid embedded in an expanding background along all three axes, taking into account both the ellipsoid's self-gravity and the external tidal field. Following Bond & Myers, we assume that each axis freezes out at a constant fraction of its initial radius, so that the mean overdensity of the collapsed object is just the same as that in the spherical collapse model (see Bond & Myers 1996 for details). The solid curve in Fig. 3(a) shows the mass of the pancake that forms around present day low-mass haloes, as a function of z . Remember that at earlier times these haloes have smaller masses. Also, owing to the roughly constant bias parameter, these results are almost independent of halo mass for $M \lesssim 10^{12} h^{-1} M_\odot$. As one can see, the pancake mass decreases with redshift, because the overdensity threshold for collapse is higher at higher z . At $z \sim 2$, the pancake mass is about $10^{12.5} h^{-1} M_\odot$. The solid curve in Fig. 3(b) shows the overdensity of the pancake at the time of formation. This overdensity increases with z , and is about 10 for $z = 1 - 2$. The ellipsoidal collapse model also determines the velocity along the first axis at the time of pancake formation. The gas associated with the pancake will be shocked. If we assume an adiabatic equation of state and that the shock is strong, all the kinetic energy is transformed into internal energy. We can calculate the post shock gas temperature as

$$T = \frac{3\mu V_1^2}{16k_B}, \quad (11)$$

where k_B is Boltzmann's constant, μ is the mean molecular weight, and V_1 is the velocity along the first axis at the time of shell crossing. We plot this temperature, as a function of z , as the thick solid curve in Fig. 3(c). The temperature decreases with increasing redshift because the mass of the pancake, M_p , is smaller at higher z and $V_1 \sim H_0 R_p \propto M_p^{1/3}$ where R_p is the Lagrangian radius of the pancake. At $z \sim 2$, the temperature is about $10^{5.5}$ K. Assuming that the gas overdensity is the same as that of the dark matter, we can estimate the specific entropy generated in the shock as

$$s = \frac{T}{n_e^{2/3}} = 17 \times \left(\frac{\Omega_{B,0} h^2}{0.024} \right)^{-2/3} \left(\frac{T}{10^{5.5} \text{K}} \right) \times \left(\frac{1+\delta}{10} \right)^{-2/3} \left(\frac{1+z}{3} \right)^{-2} \text{ keV cm}^2, \quad (12)$$

where we have taken $\mu = 0.6$, valid for a completely ionized medium dominated by hydrogen and helium. As shown by the solid curve in Fig. 3(d), s increases rapidly with decreasing redshift, mainly owing to the decreasing gas density. At $z \sim 2$ the resulting entropy is $s \sim 15 \text{ keV cm}^2$. For $z \lesssim 2.5$, pancake formation results in a preheated IGM with $s \gtrsim 10 \text{ keV cm}^2$, which corresponds to the value adopted in the preheating model discussed in the previous section.

The results presented here are based on the assumption that both e and p (which specify the local tidal field) take their most probable values. In reality, the tidal field around a point in a Gaussian density field must be coherent over a finite scale. Since the low-mass haloes at $z = 0$ are low peaks, typically with large values of e , it is possible that the value of e for the region around such a halo is larger than the most probable value. Without going into detailed calculations that include correlations of the tidal field on different scales, we consider an extreme case in which we set $e = 0.45$ for all M_r . This value for e is approximately equal to that for a peak with $\delta/\sigma = 1$. The thick dashed curves in the four panels of Fig. 3 show the results for this extreme model. Because the assumed value of e is larger than the most probable value, a given mass pancake forms earlier and correspondingly the overdensity of the pancake is lower. However, for $z \lesssim 3$, the change in T is less than 50% and the change of s is less than a factor of two.

The preheating by gravitational pancaking is expected to have important consequences for the subsequent accretion of gas into dark matter haloes only if the heated gas cannot cool efficiently. The cooling time of the heated gas can be written as

$$t_{\text{cool}} \sim 6.3 \Lambda_{-23}^{-1} \left(\frac{\Omega_{B,0} h^2}{0.024} \right)^{-1} \left(\frac{T}{10^{5.5} \text{K}} \right) \times \left(\frac{1+\delta}{10} \right)^{-1} \left(\frac{1+z}{3} \right)^{-3} \text{ Gyr}, \quad (13)$$

where Λ_{-23} is the cooling function in units of $10^{-23} \text{ erg sec}^{-1} \text{ cm}^3$. This time should be compared with the Hubble time,²

² Our notation is such that $\mathcal{H}(z) = 1$ for an Einstein-de Sitter Universe, which is also valid to good approximation for the Λ CDM concordance cosmology at $z \gtrsim 1$.

$$t_{\text{H}} = 5.0 \left(\frac{h}{0.7}\right)^{-1} \left(\frac{\Omega_0}{0.3}\right)^{-1/2} \left(\frac{1+z}{3}\right)^{-3/2} \mathcal{H}(z) \text{ Gyr}, \quad (14)$$

where $\mathcal{H}(z) = \Omega_0^{1/2} (1+z)^{3/2} H_0 / H(z)$ and $H(z)$ is Hubble's constant at redshift z . In Fig. 3(c), the three thin curves show the loci of $t_{\text{cool}} = t_{\text{H}}$ in the T - z plane for $\delta = 5, 10,$ and 20 , respectively. Here we have used the cooling function of Sutherland & Dopita (1993) with a metallicity of $0.01 Z_{\odot}$. Effective radiative cooling only occurs below these curves. Comparing these curves with those showing the temperature of the gas in pancakes, we see that heating by gravitational pancaking at $z \lesssim 2$ can have a significant impact on the subsequent accretion of gas into haloes that will be low mass today. At higher redshifts, however, the cooling proceeds sufficiently fast so that the IGM within the pancake can cool back to its original temperature by the time the low mass haloes within the pancake form.

Once again remember that the specific entropy generated by gravitational pancaking at $z \sim 2$ is very similar to what one needs to suppress the cold gas fraction in low-mass haloes (see §2). Thus we conclude that the preheating model discussed in the previous section, which is extremely successful at explaining both the stellar and HI mass functions, has a natural origin. One does not need to invoke any star formation or AGN activity; rather, the IGM is preheated to the required specific entropy by the same process that explains the formation of the dark matter haloes themselves.

4 DISCUSSION

4.1 Comparison with numerical simulations

In the previous sections we have argued that preheating by gravitational pancaking causes the shapes of the HI and stellar mass functions at the low mass ends to agree with observations. This begs the question as to why this effect has not already been seen in existing hydrodynamical, cosmological simulations. The short answer is that no previous simulation had the necessary resolution.

To study the effects discussed above places two different resolution constraints on simulations. First, they must be able to resolve the shocks that occur in the forming pancakes and second, they must resolve the small galaxies that form within them. The typical pancake thickness is $\sim 200h^{-1}$ kpc in comoving units, with an overdensity of about 10. In a Smoothed Particle Hydrodynamics (SPH) code, it requires $4h_s$ to resolve a shock (Hernquist & Katz 1989), where h_s is the SPH smoothing radius usually chosen so that there are 32 particles within a sphere of radius $2h_s$. Since the pancake has a shock on both sides, the absolute minimum resolution has to be at least $8h_s$ across the pancake thickness, i.e. $h_s \lesssim 25h^{-1}$ kpc. Even a shock capturing Eulerian grid or AMR code requires at least 4 grid cells across the pancake width to resolve the post-shock structure. The typical galaxy that needs to be affected has a dark halo with a circular velocity of $\sim 50 \text{ km s}^{-1}$, which corresponds to a halo mass of $\sim 10^{10} M_{\odot}$ and a virial radius of $\sim 50h^{-1}$ kpc. To marginally resolve such haloes requires at least 100 dark matter particles and hence a particle mass for the dark matter of less than $10^8 M_{\odot}$. In addition, one must have at least 2 spatial resolution elements within the virial radius and hence the spatial resolution must be at least $25h^{-1}$ kpc. In

an Eulerian code both these spatial resolution requirements are identical but in a Lagrangian code like SPH, where the spatial resolution is variable, the halo requirement is actually $(200/10)^{1/3} = 2.7$ times easier to satisfy owing to the higher overdensity.

The above resolutions have not been achieved in any published numerical simulation. The highest resolution simulation to date at $z = 0$ (Keres et al. 2005) has 128^3 gas and dark matter particles in a periodic, cubic volume of $22.22h^{-1}$ comoving Mpc on a side. At an overdensity of 10 this simulation has $h_s = 81h^{-1}$ kpc, more than 3 times too large to properly resolve the pancake thickness. In addition, the dark matter particle mass of $9 \times 10^8 M_{\odot}$ is almost an order of magnitude too large. Furthermore, the volume is really too small to evolve the simulation down to $z = 0$ and to sample enough different environments. Springel & Hernquist (2003) have a SPH simulation in a large enough volume, $100h^{-1}$ Mpc on a side with 324^3 gas and dark matter particles. However, both the spatial and mass resolution are worse than in the case of Keres et al. (2005), $143h^{-1}$ kpc and $2 \times 10^9 M_{\odot}$, respectively. Their latest unpublished simulation has 486^3 particles but still has worse spatial resolution ($96h^{-1}$ kpc) than Keres et al. (2005). In addition, the particle mass is $6 \times 10^8 M_{\odot}$, which is still six times too large. The Eulerian simulation of Kang et al. (2005b) has 1024^3 cells in the same size volume as Springel & Hernquist (2003) for a grid cell size of $97h^{-1}$ kpc, again worse than Keres et al. (2005). Finally, Nagamine et al. (2001) have 768^3 cells within a volume of $25h^{-1}$ comoving Mpc on a side with a spatial resolution of $75h^{-1}$ kpc.

To perform a cosmological SPH simulation in a uniform periodic volume large enough to evolve robustly to $z = 0$, i.e. $100h^{-1}$ Mpc on a side, and marginally resolve preheating, as outlined above, would require 1860^3 dark matter and gas particles. Such a large simulation is well beyond the reach of the current generation of computers and codes. However, one can reach such high resolutions in a large volume by using a ‘‘zoom-in’’ strategy, in which the resolution is only high in the region of interest (Katz & White 1993). Here, one starts with a large volume simulated at moderate resolution, identify the object whose formation one wishes to study, trace the particles that end up in or near this object back to the initial conditions, replace the particles in this Lagrangian region with a finer grid of less massive particles, add the small scale waves that can be resolved by this finer grid to the initial fluctuation spectrum, and re-run the simulation. The particle density away from the region of interest is reduced by sparse sampling the original particle grid in a series of nested zones, always keeping the particle density high enough to maintain an accurate representation of tidal forces. This approach is similar to the one used by other groups (e.g. Navarro & Steinmetz 1997, 2000; Steinmetz & Navarro 1999, Navarro et al. 1995; Sommer-Larsen et al. 1999, Robertson et al. 2004, Governato et al. 2004) in their simulations of individual galaxies but one needs to focus on present day low mass galaxies that form within pancakes at higher redshift. To test our predictions regarding the preheating by gravitational pancaking we plan to carry out investigations along this line in the near future.

4.2 Implications for galaxy formation and the IGM

According to the results presented above, the assembly of gas into galaxy-sized haloes is expected to proceed in two different modes with a transition at $z \sim 2$. At $z > 2$, the accreted intergalactic gas is cold. Since radiative cooling is efficient in galaxy haloes, gas assembly into galaxies is expected to be rapid and to be dominated by clumps of cold gas. Combined with the fact that the formation of galaxy-sized dark matter haloes at $z \gtrsim 2$ is dominated by major mergers (e.g. Li et al. 2005), this suggests that during this period gas can collapse into haloes quickly to form starbursts and perhaps also feed active galactic nuclei (e.g. Baugh et al. 2005). Galactic feedback associated with such systems may drive strong winds into the IGM, contaminating the IGM with metals. Note that strong feedback in this phase is required to reduce the star formation efficiency in high- z galaxies; otherwise too much gas would already turn into stars at high z . This phase of star formation maybe what is observed as Lyman-break galaxies and sub-mm sources at $z \gtrsim 2$, and maybe responsible for the formation of elliptical galaxies and the bulges of spiral galaxies. At $z \lesssim 2$, however, the situation is quite different. Since the medium in which galaxy-sized haloes form is already heated by previrialization and since radiative cooling is no longer efficient, the accretion is expected to be dominated by hot, diffuse gas. Such gentle accretion of gas might be favorable for the formation of the quiescent disks of spiral galaxies. Because the accreted gas is diffuse rather than in cold clumps, it can better retain its angular momentum as it settles into a rotationally supported disk. In addition, since the baryonic mass fraction that forms the disk is significantly smaller than the universal baryon fraction, the disk is less likely to become violently unstable. Both effects may help alleviate the angular momentum problem found in some numerical simulations, i.e. disks that form in CDM haloes have too little angular momentum and are too concentrated (Navarro & Steinmetz 1997).

Depending on the halo formation history, the bulge-to-disk ratio will vary from system to system. For haloes that have assembled large amounts of mass before preheating, the galaxies that form within them should contain significant bulges, while in haloes that form after preheating the galaxies should be dominated by a disk component. Since haloes that form later are less concentrated, this model naturally explains why later-type galaxies usually have more slowly rising rotation curves. An extreme example would be low-surface brightness (LSB) galaxies. By definition, LSB galaxies are disks in which the star formation efficiency is low. These galaxies are also gas rich, have high specific angular momenta, and show slowly rising rotation curves. The last two properties are best explained if LSBs are hosted by haloes that have formed only in the recent past, since such haloes have low concentrations (e.g. Bullock et al. 2001; Wechsler et al. 2002; Zhao et al. 2003a,b), and high spin parameters (e.g. Maller, Dekel & Somerville 2002; D’Onghia & Burkert 2004; Hetzner & Burkert 2005). However, there is one problem with such a link between LSBs and newly formed dark matter haloes. Since the formation of such haloes involves major mergers, these systems are expected to produce strong starbursts rather than low-surface bright-

ness disks. This problem does not exist in our model since these haloes are expected to form in a preheated medium and gas accretion into such haloes will be smooth. It will be interesting to see if our model can predict the right number of LSB galaxies and explain the existence of extreme systems like Malin I.

Our model also opens a new avenue to understand the evolution of the galaxy population with redshift. As we argued above, star formation at $z > 2$ is expected to be dominated by starbursts associated with major mergers of gas rich systems, while star formation at $z < 2$ is expected to occur mostly in quiescent disks. This has important implications for understanding the star formation history of the universe and for understanding the evolution of the galaxy population in general. For example, our model implies a characteristic redshift, $z \sim 2$, where both the star formation history and galaxy population make a transition from a starburst-dominated mode to a more quiescent mode. Furthermore, if AGNs are driven by gas-rich major mergers, a transition at $z \sim 2$ is also expected in the AGN population. There are some hints about such transitions in the observed star formation history (e.g. Blain et al. 1999), and in the observed number density of AGNs (e.g. Shaver et al. 1996). Recent observations of damped Lyman alpha systems also suggests a change in behavior at $z \sim 2$ both in the cold gas content and in the number density of such systems (see Rao 2005).

The preheated medium we envision here is closely related to the warm-hot intergalactic medium (WHIGM) under intensive study in recent years. Hydrodynamical simulations show that between 30 and 40 percent of all baryons reside in this WHIGM, which is produced by shocks associated with gravitational collapse of pancakes and filaments (e.g. Cen & Ostriker 1999; Dave et al. 2001; Kang et al. 2005b). These results are consistent with observational estimates based on the study of UV absorption lines in the spectra of low-redshifts QSOs (see Tripp et al. 2004 for a review). In our model, the low-temperature component of this WHIGM, i.e. with temperatures of a few times 10^5 K, is associated with pancakes of relatively low mass ($\sim 5 \times 10^{12} h^{-1} M_\odot$), within which late-type galaxies form. As we discussed in §4.1, current simulations are still unable to make accurate predictions regarding this particular component of the WHIGM. Future simulations of higher resolution, however, may shed light on the relation between the properties of galaxies and those of the IGM in their immediate surroundings. Such a relationship may prove pivotal in observational hunts for the missing baryons as the spatial distribution of galaxies and their properties can serve as guideposts in the search for the WHIGM.

5 CONCLUSIONS

Understanding the shallow faint-end slope of the galaxy luminosity function, or equivalently the stellar mass function, is a well known problem in galaxy formation. In the standard model it is often assumed that supernova feedback keeps large fractions of the baryonic material hot, thus suppressing the amount of star formation. Although the efficiency of this process might be tuned so that one fits the faint-end slope of the galaxy luminosity function it has a number

of problems. First, the required efficiencies are extremely high and are inconsistent with detailed numerical simulations (e.g., Mac-Low & Ferrara 1999). Second, unless the hot gas is somehow expelled from the dark matter halo forever, which requires even higher feedback efficiencies, this model predicts hot haloes of X-ray emitting gas around disk galaxies, which is inconsistent with observations (e.g., Benson et al. 2000). In this paper we have demonstrated that this model has an additional shortcoming. Using recently obtained HI mass functions we show that the supernova feedback model predicts HI masses that are too high. The reason is that supernova feedback requires star formation which in turn requires high surface densities of cold gas. The latter owes to the existence of a star formation threshold density, which has strong support from both theory (e.g., Quirk 1972, Silk 2001) and observations (e.g., Kennicutt 1989; Martin & Kennicutt 2001).

We therefore argue that simultaneously matching the shallow, low-mass slopes of the stellar and HI mass functions requires an alternative mechanism, which does not directly depend on star formation. We demonstrate that a mechanism that can preheat the IGM to a specific gas entropy of $\sim 10 \text{ keV cm}^2$, can fit both the observed stellar mass function as well as the HI mass function. We also show that gravitational instability of the cosmic density field can be the source of this preheating. Our idea is fairly simple: low mass haloes form within larger-scale overdensities that have already undergone collapse along their first axis. This ‘pancake’ formation causes the associated gas to be shock-heated, and providing that the gas cooling rate is sufficiently slow, the low mass haloes embedded within these pancakes subsequently form in a preheated medium.

Using the ellipsoidal collapse model, we demonstrate that the progenitors of present-day haloes with masses $M \lesssim 10^{12} h^{-1} M_{\odot}$ were embedded in pancakes of masses $\sim 5 \times 10^{12} h^{-1} M_{\odot}$ at $z \sim 2$. The formation of such pancakes can heat the gas associated with them to a temperature of $\sim 5 \times 10^5 \text{ K}$ and compress it to an overdensity of ~ 10 . This gas has a cooling time longer than the age of the Universe and a specific entropy of about 15 keV cm^2 ; the amount needed to explain the observed stellar and HI mass functions.

Our results demonstrate that heating associated with previrialization may also help solve a number of outstanding problems in galaxy formation within a CDM universe. However, detailed, high-resolution numerical simulations will be required to test our predictions in detail. Such simulations will help us understand how the formation of a pancake heats the gas initially associated with it and whether the amount of heating follows our analytic results. For example, our calculation indicates that shock heating will dominate over cooling in typical pancakes at $z \lesssim 2$. However, such calculations assume that the gas is smoothly distributed. Structures at scales smaller than the pancake could lead to density inhomogeneities, either pancakes, filaments or halos, and these could promote extra cooling and move the transition to lower redshifts. A similar effect occurs when one calculates the transition mass from cooling dominated to infall dominated accretion in galaxy formation (White & Frenk 1992) and compares it with actual simulations (Keres et al 2005). They will also help us understand how such heating affects subsequent gas accretion and cooling into

the dark haloes that form in the pancake and hopefully derive actual stellar and HI mass functions at the small mass end. We have argue that no cosmological, hydrodynamical simulation to date has the required spatial and/or mass resolution to study the pancake preheating proposed here. To achieve the required numerical resolution, we suggest resimulating, at high resolution, a number of pancakes (and filaments) with masses of the order of $5 \times 10^{12} h^{-1} M_{\odot}$, identified from large cosmological, hydrodynamical simulations. Thus far this ‘zoom-in’ strategy has mainly been used to study clusters and galaxies. If our estimates are correct, it will be extremely interesting to apply this technique to study pancakes and their enclosed, low mass haloes.

ACKNOWLEDGEMENT

We thank Jessica Rosenberg and Martin Zwaan for providing us with their HI mass functions. FvdB is grateful to Aaron Dutton, Justin Read and Greg Stinson for valuable discussion. NSK was supported by NSF AST-0205969, NASA NAGS-13308, and NASA NNG04GK68G.

REFERENCES

- Babul A., Rees M.J., 1992, MNRAS, 539, 517
 Baugh C. M., Lacey C. G., Frenk C. S., Granato G. L., Silva L., Bressan A., Benson A. J., Cole S., 2005, MNRAS, 356, 1191
 Bell E.F., McIntosh D.H., Katz N., Weinberg M.D., 2003, ApJ, 585, 117
 Bardeen J.M., Bond J.R., Kaiser N., Szalay A.S., 1986, ApJ, 304, 15
 Benson A.J., Bower R.G., Frenk C.S., White S.D.M., 2000, MNRAS, 314, 557
 Benson A.J., Lacey C.G., Baugh C.M., Cole S., Frenk C.S., 2002, MNRAS, 333, 156
 Benson A.J., Bower R.G., Frenk C.S., Lacey C.G., Baugh C.M., Cole S., 2003, ApJ, 599, 38
 Berlind A.A., et. al., 2003, ApJ, 593, 1
 Blain A.W., Smail I., Ivison R.J., Kneib J.P., 1999, MNRAS, 302, 632
 Blumenthal G.R., Faber S.M., Primack J.R., Rees M.J., 1984, Nature, 311, 517
 Bond J.R., Myers S.T., 1996, ApJS, 103, 1
 Boselli A., Lequeux J., Gavazzi G., 2002, A&A, 384, 33
 Bullock J.S., Kravtsov A.V., Weinberg D.H., 2000, ApJ, 539, 517
 Bullock J.S., Kolatt T.S., Sigad Y., Somerville R.S., Klypin A.A., Primack J.R., Dekel A., 2001a, MNRAS, 321, 559
 Bullock J.S., Dekel A., Kolatt T.S., Kravtsov A.V., Klypin A.A., Porciani C., Primack J.R., 2001b, ApJ, 555, 240
 Cen R., Ostriker J.P., 1999, ApJ, 514, 1
 Cole C., Lacey C.G., 1996, MNRAS, 281, 716
 Cole C., Lacey C.G., Baugh C.M., Frank C.S., 2000, MNRAS, 319, 168
 Colless M., The 2dFGRS team, 2001, MNRAS, 328, 1039
 Cooray A., Milosavljević M., 2005, preprint (astro-ph/0504580)
 Croft R.A.C., Weinberg D.H., Pettini M., Hernquist L., Katz N., 1999, ApJ, 520, 1
 Dave R., et al., 2001, ApJ, 552, 473
 Dekel A., Silk J., 1986, ApJ, 303, 39
 D’Onghia E., Burkert A., 2004, ApJ, 612, L13
 Doroshkevich A.G., 1970, Astrofizika, 3, 175
 Efstathiou G., 1992, MNRAS, 256, 43
 Fall S.M., Efstathiou G., 1980, MNRAS, 193, 189
 Garnett D.R., 2002, ApJ, 581, 1019

- Gnedin N.Y., 2000, *ApJ*, 542, 535
- Governato F., Mayer L., Wadsley J., Gardner J.P., Willman B., Hayashi E., Quinn T., Stadel J., Lake, G., 2004, *ApJ*, 607, 688
- Heckman T.M., Lehnert M.D., Strickland D.K., Armus L., 2000, *ApJS*, 129, 493
- Hetznecker H., Burkert A., 2005, *astro-ph/0505249*
- Hoeft M., Yepes G., Gottloeber S., Springel V., 2005, preprint (*astro-ph/0501304*)
- Hunter D.A., Elmegreen B.G., Baker A. L., 1998, *ApJ*, 493, 595
- Jesseit R., Naab T., Burkert A., 2002, *ApJ*, 571, L89
- Jing Y.P., 1999, *ApJ*, 515, 45
- Kang X., Jing Y.P., Mo H.J., Börner G., 2005, *ApJ*, in press (*astro-ph/0408475*)
- Kang H., Ryu D., Cen R., Song D., 2005b, *ApJ*, 620, 21
- Katz N., White S.D.M., 1993, *ApJ*, 412, 455
- Katz N., Quinn T., Bertschinger E., Gelb J.M., 1994, *MNRAS*, 270, L71
- Kauffmann G., et al. 2003, *MNRAS*, 341, 33
- Kauffmann G., Colberg J.M., Diaferio A., White S.D.M., 1999, *MNRAS*, 303, 188
- Kauffmann G., White S.D.M., Guiderdoni B., 1993, *MNRAS*, 264, 201
- Kennicutt R.C., 1989, *ApJ*, 344, 685
- Kennicutt R.C., 1998, *ApJ*, 498, 541
- Keres D. Yun M.S., Young J.S., 2003, *ApJ*, 582, 659
- Keres D., Katz N., Weinberg D.H., Dave R., 2004, preprint (*astro-ph/0407095*)
- Kraan-Korteweg R.C., van Driel W., Briggs F., Bingelli B. Mostefaoui T.I., 1999, *A&AS*, 135, 255
- Lewis G.F., Babul A., Katz N., Quinn T., Hernquist L., Weinberg D.H., 2000, *ApJ*, 536, 623
- Li Y., Mo H.J., van den Bosch F.C., 2005, *MNRAS*, in preparation
- Mac Low M.M., 1999, *ApJ*, 524, 169
- Mac Low M.M., Ferrara A., 1999, *ApJ*, 513, 142
- McGaugh S.S., de Blok W.J.G., 1997, *ApJ*, 481, 689
- Maller A.H., Dekel A., Somerville R., 2002, *MNRAS*, 329, 423
- Martin C.L., 1999, *ApJ*, 513, 156
- Martin C.L., Kennicutt R.C., 2001, *ApJ*, 555, 301
- Mo H.J.; Mao S., 2002, *MNRAS*, 333, 768
- Mo H.J.; Mao S., White S.D.M., 1998, *MNRAS*, 295, 319
- Mo H.J.; White S.D.M., 1996, *MNRAS*, 282, 347
- Mo H.J.; White S.D.M., 2002, *MNRAS*, 336, 112
- Nagamine K., Fukugita, M., Cen R., Ostriker J.P., 2001, *ApJ*, 558, 497
- Narayanan V.K., Spergel D.N., Dave R., Ma C., 2000, *ApJ*, 543, L103
- Navarro J.F., Steinmetz M., 1997, *ApJ*, 478, 13
- Navarro J.F., Steinmetz M., 2000, *ApJ*, 538, 477
- Navarro J.F., Frenk C.S., White S.D.M., 1995, *MNRAS*, 275, 720
- Navarro J.F., Frenk C.S., White S.D.M., 1997, *ApJ*, 490, 493
- Oh S.P., Benson A.J., 2003, *MNRAS*, 342, 664
- Panther B., Heavens A.F., Jimenez R., 2004, *MNRAS*, 355, 764
- Peebles P.J.E., 1990, *ApJ*, 365, 27
- Quinn T., Katz N., Efstathiou G., 1996, *MNRAS*, 278, L49
- Quirk W.J., 1972, *ApJ*, 176, L9
- Rao S., 2005, in P. Williams et al. eds. Probing galaxies through quasar absorption lines, IAU Colloquium 199, Cambridge Univ. Press.
- Rees M.J., 1986, *MNRAS*, 218, P25
- Robertson B., Yoshida N., Springel V., Hernquist L., 2004, *ApJ*, 606, 32
- Rosenberg J.L., Schneider S.E., 2002, *ApJ*, 567, 247
- Schechter P., 1976, *ApJ*, 203, 297
- Schneider S.E., Spitzak J.G., Rosenberg J.L., 1998, *ApJ*, 507, L9
- Seljak U., McDonald P., Makarov A., 2003, *MNRAS*, 342, L79
- Seljak U., Warren M.S., 2004, *MNRAS*, 355, 129
- Shaver P.A., Wall J.V., Kellermann K.I., Jackson C.A., Hawkins M.R.S., 1996, *Nat*, 384, 439
- Sheth R.K., Tormen G., 1999, *MNRAS*, 308, 119
- Sheth R.K., Mo H.J., Tormen G., 2001, *MNRAS*, 323, 1
- Silk J., 2001, *MNRAS*, 324, 313
- Sommer-Larsen J., Gelato S., Vedel H., 1999, *ApJ*, 519, 501
- Somerville R.S., Primack J.R., 1999, *MNRAS*, 310, 1087
- Spergel D.N., et al., 2003, *ApJS*, 148, 175
- Springel V., Hernquist L., 2003, *MNRAS*, 339, 289
- Springel V., White S.D.M., Tormen G., Kauffmann G., 2001, *MNRAS*, 328, 726S
- Steinmetz M., Navarro J.F., 1999, *ApJ*, 513, 555
- Strickland D.K., Stevens I.R., 2000, *MNRAS*, 314, 511
- Sutherland R., Dopita M., 1993, *ApJS*, 88, 253
- Thoul A.A., Weinberg D.H., 1996, *ApJ*, 465, 608
- Tinker J., Weinberg D.H., Zheng Z., Zehavi I., 2004, preprint (*astro-ph/0411777*)
- Toomre A., 1964, *ApJ*, 139, 1217
- Tremonti C.A., et al., 2004, *ApJ*, 613, 898
- Tripp T., Bowen D.V., Sembach K.R., Jenkins E.B., Savage B.D., Richter P., 2004, *astro-ph/0411151*
- Tully R.B., Somerville R.S., Trentham N., Verheijen M.A.W., 2002, *ApJ*, 569, 573
- van den Bosch F.C., 2000, *ApJ*, 530, 177
- van den Bosch F.C., 2001, *MNRAS*, 327, 1334
- van den Bosch F.C., 2002, *MNRAS*, 332, 456
- van den Bosch F.C., Abel T., Croft R.A.C., Hernquist L., White S.D.M., 2002, *ApJ*, 576, 21
- van den Bosch F.C., Abel T., Hernquist L., 2003a, *MNRAS*, 346, 177
- van den Bosch F.C., Yang X.H., Mo H.J., 2003b, *MNRAS*, 340, 771
- van den Bosch F.C., Yang X.H., Mo H.J., Norberg P., 2005, *MNRAS*, 356, 1233
- Warren M.S., Quinn P.J., Salmon J.K., Zurek W.H., 1992, *ApJ*, 399, 405
- Wechsler R.H., Bullock J.S., Primack J.R., Kravtsov A.V., Dekel A., 2002, *ApJ*, 568, 52
- Weinmann S.M., van den Bosch F.C., Yang X., Mo H.J., Li C., Jing Y.P., 2005, in preparation
- White S.D.M., Frenk C.S., 1991, *ApJ*, 379, 52
- White S.D.M., Rees M.J., 1978, *MNRAS*, 183, 341
- Wong T., Blitz L., 2002, *ApJ*, 569, 157
- Yang X.H., Mo H.J., van den Bosch F.C., 2003, *MNRAS*, 339, 1057
- Yang X.H., Mo H.J., Jing Y.P., van den Bosch F.C., Chu Y. 2004, *MNRAS*, 350, 1153
- Yang X.H., Mo H.J., Jing Y.P., van den Bosch F.C., 2005, *MNRAS*, 358, 217
- Zasov A.V., Smirnova A.A., 2005, *Astron. Lettters*, 31, 160
- Zel'dovich Y. B., 1970, *A&A*, 5, 84
- Zhao D.H., Mo H.J., Jing Y.P., Börner G. 2003a, *MNRAS*, 339, 12
- Zhao D.H., Jing Y.P., Mo, H.J., Boerner G., 2003b, *ApJ*, 597, L9
- Zwaan M.A., et al. 2003, *AJ*, 125, 2842
- Zwaan M. A., Meyer M. J., Staveley-Smith L., Webster R. L., 2005, *astro-ph/0502257 (Z05)*